

RAMAN LIDAR FOR SYNCHRONOUS WATER VAPOR, LIQUID WATER AND ICE WATER PROFILINGS

Wang Yufeng, Zhang Jing, Wang Qing, Gao Fei, Di Huige, He Tingyao, Yan Qing, Liu Jingjing, Hua Dengxin

School of Mechanical and Precision Instrument Engineering, Xi'an University of Technology, Xi'an 710048, China

Email: wangyufeng@xaut.edu.cn

ABSTRACT

Water is the only atmospheric parameter with three-phase state. An ultraviolet Raman lidar was developed for synchronous measurements for water vapor, liquid water and ice water in Xi'an University of Technology, Xi'an, China (34.233°N, 108.911°E). An accurate retrieval method on the basis of interference degree is proposed for synchronous three-phase water mixing ratio profiles. Preliminary measurements are carried out in the Laser Radar Center of Remote Sensing of Atmosphere (LRCRSA). Several representative examples are obtained and validated the performance of Raman system. Combined with atmospheric temperature profiles, the synchronous water vapor, liquid water and ice water profiling are retrieved and revealed the variation characteristics in three-phase water. The effective detection can reach up to a height of 5 km under cloudy weather, and synchronized growth in water vapor and liquid water content was obtained in cloud layers. Continuous observations are also made under haze weather condition, and the temporal and spatial evolution trend of three-phase water in clouds at 2 km altitude are successfully realized.

Keywords: Raman lidar, water vapor, liquid water.

1. INTRODUCTION

Water vapor is the only atmospheric parameter with three-phase state, which plays an important role in the global water cycle. Water vapor plays an important role in cloud evolution, precipitation and climate change. Liquid water in clouds is not only an important component in the balance of atmospheric water budget, but also an important microphysical parameter to understanding cloud physical processes. Super-cooled water in cloud (which remains liquid below 0° C), is also one of the most important

parameters indicative to the potential of artificial precipitation enhancement. Therefore, the study of water three-phase distribution with high precision and high-spatial-temporal resolution is of great significance in understanding the formation of cloud and precipitation, fine analysis and prediction of precipitation, and artificial precipitation enhancement.

Lidar is a powerful tool in the remote sensing of atmospheric components and atmospheric properties. Many ground-based Raman lidar systems have achieved currently exist around the world, and significant achievements have been made in the measurement of atmospheric water vapor and aerosol profiles [1-4]. Recent years, several institutes have carried out research work on three-phase water. In 2000, Veselovski et.al developed a Raman lidar for detecting water vapor and liquid water in tropospheric layer, and the relative lidar power under different atmospheric conditions was mainly discussed [5]. In 2004, Zhien Wang et.al developed a Raman lidar to detect the solid-water content in cirrus clouds, and proposed the inversion method of solid-water mixing ratio [6]. In 2012, Yi Fan et.al obtained complete Raman spectra of three-phase water by a 32-channel grating spectrometer, and achieved lidar returned signals of atmospheric water vapor and liquid water in the range of 0-6 km [7]. It is required to further studies on synchronous detection, especially on synchronous retrievals of accurate mixing ratio profiling.

In this paper, an ultraviolet Raman lidar system has been established for synchronous measurement of atmospheric three-phase water. We also carried out preliminary experiments to validate the performance of Raman lidar under different weather condition. Furthermore, an accurate retrieval method on the basis of interference degree is proposed for synchronous three-phase water mixing ratio profiles. The

results show that the synchronous detection of atmospheric three-phase water below 5 km can be realized, and the synchronous growth of liquid water and water vapor in clouds is achieved.

2. METHODOLOGY

2.1 The Raman lidar system

The ultraviolet Raman lidar system used in this study was developed at Xi'an University of Technology. A schematic diagram of the system is presented in Fig. 1. A set of dichroic mirrors (DMs) and narrow-band interference filters (IFs) is used to construct a high-efficiency polychromator, which divides the returned signals into five channels: channel 1 is used for the detection of elastic Mie-Rayleigh signals, at central-wavelength of 354.7nm; channel 2-5 are used for the detection of different vibrational Raman scattering signals; channel 2 is for vibrational Raman lidar returns with a central-wavelengths of 386.7 nm; and channel 3-5 are used to detect Raman scattering signals of ice water, liquid water and water vapor molecules, with central-wavelengths of 397.0nm, 403.0nm and 407.6 nm, respectively.

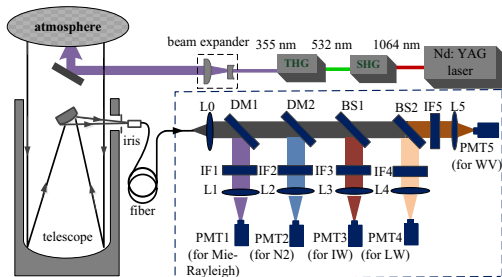


Fig.1 Diagram of Raman lidar for synchronous three-phase water detection. DM: Dichroic Mirror, IF: Interference Filters, BS: Beam Splitter.

2.2 Retrieval methods

According to its definition, three-phase water mixing ratio can be retrieved by using the ratio of Raman scattering signals of three-phase water and nitrogen molecules, and can be given as,

$$\begin{cases} W_{WV}(z) = 0.485 \times \frac{P_{WV}(z)}{P_N(z)} \cdot \frac{k_N}{k_{WV}} \cdot \frac{\sigma_N(\pi)}{\sigma_{WV}(\pi)} \cdot \exp\left\{\int_0^z [\alpha_{WV}(z') - \alpha_N(z')] dz'\right\} \\ W_{LW}(z) = \frac{P_{LW}(z) - C_{LW} P_{WV}(z) - C_{LW} P_{IW}(z)}{P_N(z)} \cdot \frac{k_N \sigma_N(\pi)}{k_{LW} \sigma_{LW}(\pi)} \cdot \exp\left\{\int_0^z [\alpha_{LW}(z') - \alpha_N(z')] dz'\right\} \\ -f_{AE} \frac{1}{\Delta Z_{CB}} \times \int_{z_{CB}-\Delta z}^{z_{CB}} \frac{P_{LW}(z') - C_{LW} P_{WV}(z')}{P_N(z')} \exp\left\{\int_{z_{CB}-\Delta z}^{z_{CB}} [\alpha_{LW}(z') - \alpha_N(z')] dz'\right\} dz' \\ W_{IW}(z) = \frac{P_{IW}(z) - C_{IW} P_{LW}(z)}{P_N(z)} \cdot \frac{k_N \sigma_N(\pi)}{k_{IW} \sigma_{IW}(\pi)} \cdot \exp\left\{\int_0^z [\alpha_{IW}(z') - \alpha_N(z')] dz'\right\} \end{cases}$$

where the subscripts LW, WV, IW and N denote liquid water, water vapor, ice water and N2

molecules, respectively. P is the output power of the channel, σ is the cross section of Raman scattering, α_i is the extinction coefficient at the wavelength λ , k is the system efficiency factor, including the optical efficiency and electrical efficiency of system. C represents the interference degree from different water phase Raman channels. Thus, due to spectral overlap characteristics of three-phase water, it is essential to take into account mutual interference degree of different phase water, to achieve synchronous retrieval of three-phase water.

3. MEASUREMENTS EXAMPLES AND RESULTS

The Raman lidar system was built and operated at Xi'an University of Technology, Xi'an (34.233°N, 108.911°E), China. Some tests were conducted to validate the system performance. Figure 2 presented two representative measurement examples taken at under cloudy condition. The left figure corresponds to the results taken at 21:39 CST on 29 Sep, 2018. Two obvious peaks appear at heights of 4.5 km and 5.5 km from the elastic scattering signals. The effective range can reach 6km and 5km for water vapor and liquid water Raman channel, and synchronous grow of water vapor and liquid water in the clouds can be observed. Another measurement example was taken at 22:35 CST on March 4, 2019, as shown in right figure. Two obvious peaks appear at heights of 1-1.2 km (cloud 1) and 2-2.2 km (cloud 2) from the elastic scattering signals, which correspond to the information of thin cloud layers. Fortunately, we can obviously synchronous increase in the RSCS of water vapor, liquid water and ice water in cloud layer 1 of ~1.2km. At the heights of 2-2.2km of cloud layer 2, synchronous growth can also be observed in water vapor and liquid water, however, it has failed to capture the information in ice water because of the weak signal itself, indicating that the Raman lidar system has successfully realized the simultaneous detection of atmospheric water vapor, liquid water and ice water in the clouds.

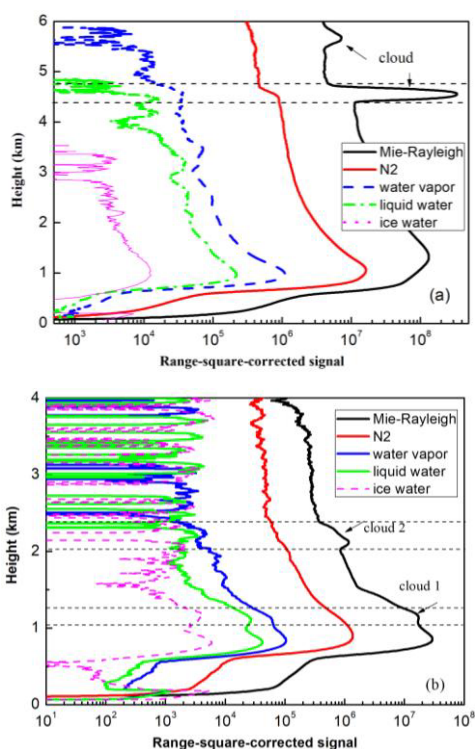


Fig.2 Representative measurement examples under cloudy weather condition. (a) Range-square-corrected signal taken at 21:39 CST on 29 Sep, 2018. (b) Range-square-corrected signal taken at 22:35 CST on March 4, 2019.

Another measurement example was taken at 23:54 CST on December 24, 2018, as shown in Fig.3. The example is also used to validate the performance of the Raman lidar under haze weather condition. The local ground temperature is 4 °C, and the visibility is 5 km, and the concentration of PM 2.5 and PM10 are 75 $\mu\text{g}/\text{m}^3$ and 145 $\mu\text{g}/\text{m}^3$ by , respectively, AQI is 99, indicating mild haze weather. From the RSCS of Mie-Rayleigh scattering signals, there exists a thick cloud layer at heights of 1.8-2.1 km, and thus the effective detection range can only reach 2 km. Meanwhile, the cloud information does not appear in the attenuated nitrogen vibrational Raman signals, which verifies the high rejection rate to elastic scattering signals. The retrieval mixing ratio of three-phase water profiles are also shown at the right. Evident enhancement of water vapor, liquid water and ice water can be obtained at the cloud layer.

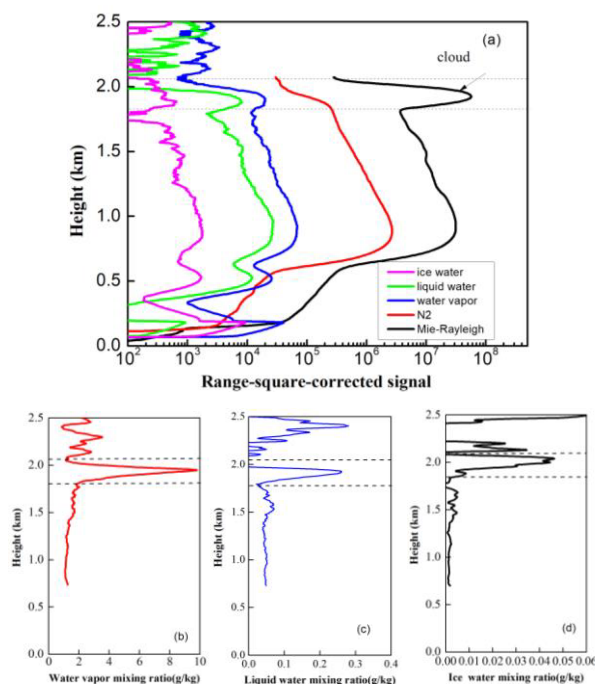


Fig. 3 Measurement results taken at 23:54 CST on December 24, 2018 under mild haze and cloud condition. (a)Range-square-corrected signal, (b)water vapor mixing ratio, (c)liquid water mixing ratio and (d)ice water mixing ratio.

ACKNOWLEDGEMENTS

This work was supported by the National Natural Science Foundation of China (NSFC) (grant No. U1733202, 41627807, 41575027 and 41027004).

REFERENCES

- [1] M. Froidevaux., et al. *Advances in Water Resources*, 51, 345-356 (2013)
- [2] T. Leblanc., et al. *Atmos. Meas. Tech.* 5, 17-36 (2012)
- [3] Wang Yufeng, et al. *Journal of Quantitative Spectroscopy and Radiative Transfer*, 205, 114-126 (2018)
- [4] A. Behrendt., et al. *Appl. Opt.*, 41(36), 7657-7666 (2002)
- [5] Veselovskii I A, et al. *Applied Physics B*, 71(1):113-117(2000)
- [6] Wang Z, et al. *Geophysical Research Letters*, 31(311):121-141(2001).